JPRS-CST-84-016

6 June 1984

China Report

SCIENCE AND TECHNOLOGY

FBIS FOREIGN BROADCAST INFORMATION SERVICE

REPRODUCED BY
NATIONAL TECHNICAL
INFORMATION SERVICE
U.S. DEPARTMENT OF COMMERCE
SPRINGFIELD, VA. 22161

NOTE

JPRS publications contain information primarily from foreign newspapers, periodicals and books, but also from news agency transmissions and broadcasts. Materials from foreign-language sources are translated; those from English-language sources are transcribed or reprinted, with the original phrasing and other characteristics retained.

Headlines, editorial reports, and material enclosed in brackets [] are supplied by JPRS. Processing indicators such as [Text] or [Excerpt] in the first line of each item, or following the last line of a brief, indicate how the original information was processed. Where no processing indicator is given, the information was summarized or extracted.

Unfamiliar names rendered phonetically or transliterated are enclosed in parentheses. Words or names preceded by a question mark and enclosed in parentheses were not clear in the original but have been supplied as appropriate in context. Other unattributed parenthetical notes within the body of an item originate with the source. Times within items are as given by source.

The contents of this publication in no way represent the policies, views or attitudes of the U.S. Government.

PROCUREMENT OF PUBLICATIONS

JPRS publications may be ordered from the National Technical Information Service, Springfield, Virginia 22161. In ordering, it is recommended that the JPRS number, title, date and author, if applicable, of publication be cited.

Current JPRS publications are announced in Government Reports Announcements issued semi-monthly by the National Technical Information Service, and are listed in the Monthly Catalog of U.S. Government Publications issued by the Superintendent of Documents, U.S. Government Printing Office, Washington, D.C. 20402.

Correspondence pertaining to matters other than procurement may be addressed to Joint Publications Research Service, 1000 North Glebe Road, Arlington, Virginia 22201.

JPRS-CST-84-016

6 June 1984

CHINA REPORT
SCIENCE AND TECHNOLOGY

CONTENTS

PEOPLE'S REPUBLIC OF CHINA

APPLIED SCIENCES

LIFE SCIENCES

ABSTRACTS

MICROBIOLOGY

APPLIED SCIENCES

INTENSIVE GEOLOGICAL WORK PRECEDES NUCLEAR POWER PLANT SITE SELECTION

Hangzhou ZHEJIANG RIBAO in Chinese 16 Apr 84 p 1

[Text] In early April, preliminary geological survey work began on the Huadong Nuclear Power Plant, the second such plant the State plans to build in Zhejiang Province.

The design power of this nucelar power plant will be twice that of the Qinshan facility. After this major national construction project is finished, even more energy will be made available for the development of the Shanghai Economic Zone. The overall geological and engineering geological surveys are being handled by the Provincial Geological Minerals Bureau. This bureau drew up detailed geological work plans and quickly assembled personnel from eight geological and specialized brigades (representing hydrography, engineering geology, geophysical surveying, cartography, and regional geological survey, etc.) to form a specialized grass-roots unit. A senior engineer was appointed as the unit's chief engineer. He was provided with 25 engineers and assistant engineers. The bureau's leadership also went to the work site to make on-the-spot studies and arrangements. In order to accelerate progress, geological personnel who had just gone to the unit braved rain to carry out all kinds of field survey work, including geophysical exploration, cartographic work, and hydrological and geological surveys. Initial progress has now been realized. The aerial geophysical and magnetic survey teams of the Provincial Geological Minerals Bureau will soon undertake aerial magnetic survey missions.

CSO: 4008/295

ANALYSIS OF TOKAMAK CONDITIONING TECHNIQUES

Chongqing HEJUBIAN YU DENGLIZITI WULI [NUCLEAR FUSION AND PLASMA PHYSICS] in Chinese No 2, 1983 pp 65-71

[Article by Yao Lianghua [1202 5328 7520], Southwest Institute of Physics:
"Analysis of Tokamak Conditioning Techniques and Their Mechanisms"]

[Summary] Tokamak conditioning techniques are intended to prevent impurities in the container walls from affecting the plasma. In the Taylor method, continuous cleaning is performed with an audio-frequency discharge, resulting in removal of carbon impurities and a lowering of oxygen to less than 1 percent of the atoms in the monoatomic layer.

Electron energy is plotted against electron temperature for various types of discharges. "We believe that in the Taylor-method discharge the electron density in the gas is between that for a glow discharge and an arc discharge and that a few percent of the gas consists of ions, while the electron temperature is in the range for a glow discharge. Discharge physics indicates that the Taylor cleaning discharge is equivalent to a high-ionization (or high-current-density) glow discharge. At a sufficiently low working pressure (10^{-4} Torr), a rather low ionization rate ($n_{H^+}/n_{H_2} < 10\%$), and with T_e 3 eV, the main process in a hydrogen discharge is elastic and inelastic collision between electrons and gas molecules.... Therefore we may make the simplified assumption that in the process of transport produced by the electric field, electrons continually collide elastically and inelastically with relatively static gas molecules and are heated up; the rate of transport of the electrons in the electric field is about one-tenth of the electron thermal movement speed, and in inelastic collisions with gas molecules they lose most of the energy obtained from the electric field."

Franck-Condon hydrogen atoms are the main types taking part in the cleaning discharge.

The average reaction rate is plotted against the electron temperature for several important reactions involving inelastic collisions between electrons and H_2. "It is evident that the reaction rate for ionization of hydrogen atoms only catches up with that for dissociation of hydrogen molecules at T_e = 12 eV. Therefore, at a low electron temperature, the main output is of hydrogen atoms and hydrogen atoms in the excited state."

"Some 30 percent of the plasma in a Tokamak discharge comes from gas liberated by the walls, while only about 70 percent is the gas injected before the discharge (depending on wall temperature and wall adsorption conditions). This indicates that in the entire discharge process, recycling between the working gas and the gas sorbed on the walls is extremely rapid and hydrogen atoms with various energies (electron charge exchange high-energy neutral particles and low-energy Franck-Condon atoms) and hydrogen ions, as well as other impurity particles, bombard the walls, penetrating and diffusing to some depth in the surface, and reacting with carbon compounds and metal oxides bound to the walls to form volatile gases such as methane, other hydrocarbons, H_2O, CO and CO_2 and the like. At high currents and in long-cycle normal tokamak discharge processes, the great majority of these volatile reaction products enter the plasma current passage and are dissociated and ionized, becoming plasma impurities. When the discharge ends, C^{n+} and O^{m+} ions interact with substances in the walls, producing reaction products which persist."

The main reactions of between metal oxides and hydrogen, particularly those of iron and titanium (which is used as an oxygen absorber) are presented.

8480
CSO: 4008/180

SECOND CRITERION FOR A THERMONUCLEAR FUSION REACTOR PRODUCING ZERO NET POWER

Chongqing HEJUBIAN YU DENGLIZITI WULI [NUCLEAR FUSION AND PLASMA PHYSICS] in Chinese No 2, 1983 pp 90-97

[Article by Wang Hongzhang [3769 7703 4545], Institute of Plasma Physics, CAS, Hefei: "Second Criterion for a Thermonuclear Fusion Reactor Producing Zero Net Power"]

[Summary] The Lawson criterion for the break-even condition in a fusion reactor is expressed in terms of the product $n\tau$ (density times confinement time) and T (the plasma temperature). "We believe that the Lawson criterion needs to be supplemented by the important quantity η_H, the overall heating efficiency of the fusion reactor, to give a correct description of the break-even condition."

"Based on the above ideal energy balance derivations and calculations we can tentatively reach the following conclusions."

"1. The first criterion (Lawson criterion) uses the two-dimensional $n\tau$-T space to describe the break-even condition for a fusion reactor, expressed as a curve in this plane. The second criterion uses a 3-dimensional space ($n\tau$, T and η_H) to describe the break-even condition, expressed as a curved surface in this space; the first break-even condition is a special case of it, consisting of a curve in this surface ($\eta_H = 1$). The second criterion can indicate the numerical values and interrelationships of the quantities involved under various conditions and is a more complete description of the break-even condition."

"2. The degree of advancement of different types of fusion devices can be compared in second-criterion graphs.... A fusion device which appears advanced in a Lawson plot may not appear so on a second-criterion plot: we must also take into account whether it is advanced in terms of η_H. The second-criterion plot gives a more correct indication of how far a given fusion device is from the ignition region.

"3. The main factors which determine reactor characteristics are the plasma temperature T, the density n, the confinement time τ, and also the overall heating efficiency η_H. The shape of the second-criterion curved surface indicates that $n\tau$ and T are also functions of η_H. Therefore, in research on thermonuclear fusion, in addition to continuing to increase $n\tau$ and T, we must also strive to increase η_H. Moreover, we also must conduct research in high-efficiency heating methods and confinement methods since this helps to further increase η_H."

"4. For a deuterion-tritium reactor with a lithium blanket the heating efficiency must be at least 1.4 percent, while that for a deuterion-tritium reactor should be at least 9 percent. If η_H is below these critical values, no matter how high the temperature or the value of $n\tau$, no reactor can realize the break-even condition. At various plasma temperatures the value of should always be greater than the corresponding critical value η_H^o."

"5. In a fusion plasma, because the electron temperature T_e produced by the heating method is greater than the ion temperature T_i, there is some effect on the break-even condition, but this effect is not entirely clear."

"6. In any real reactor the plasma temperature T and the density n have some spatially symmetrical distribution, so that the temperature and density at the center of the plasma must be sufficiently greater than the second-criterion value in order that the average temperature and density will exceed the second-criterion value."

8480
CSO: 4008/180

RADIATION PROTECTION ASSESSMENT OF CHINA'S FIRST HEAVY WATER REACTOR

Taiyuan FUSHE FANGHU [RADIATION PROTECTION] in Chinese No 5, Sep 83 pp 321-328

[Article by Zhang Yongxiang [1728 3057 4382]: "Radiation Protection Assessment of the Past 20 Years of Operation of the First Heavy Water Reactor in China"]

[Text] [Abstract] The article discusses work on radiation protection during the last 20 years of operation of a heavy water research reactor. The total collective radiation dose equivalent received by the operators was equal to 1537.59 man·rem; the average dose equivalent per person was 0.62 rem; the average "cost" of a 1 MWY reactor in terms of the collective dose was equal to 34.63 man·rem. The amount of radioactive material released into the environment was less than the permissible limit. Complete medical examinations of the workers did not reveal any diagnostic radiation injuries. Radioactive ^{60}Co generated by corrosion and wear in the first reactor loop is an important source of both internal and external radiation.

The HWRR-1, China's first experimental heavy water reactor, employs heavy water as both coolant and moderator and uses fuel rods containing 2 percent ^{235}U metal. Its peak rated power was originally 7,000 kW but was subsequently increased to 10,000 kW, which increased the maximum thermal neutron flux to $1.25 \cdot 10^{14}/sec \cdot cm^2$. In its original form the reactor was used mainly in physics experiments and to produce small amounts of isotopes. After the reactor had been upgraded to operate continuously at 10,000 kW, radiation studies of the fuel rods and materials commenced at the same time that isotope production was stepped up. During the period from 1958 to 1978, the HWRR-1 generated a total energy equal to 44.4 MWY.

Work on radiation protection has made gradual progress during these 20 years. Radiation safety has been studied on several occasions (for example, the internal and external radiation produced by radioactive materials has been monitored and estimated), and rudimentary results and a certain amount of general experience have been gained in various areas. We will discuss the following aspects of the problem: 1) individual dose monitoring and assessment of the health consequences; 2) worksite monitoring; 3) measurement of gaseous, water and solid wastes; 4) accidents; and 5) conclusions.

1. Monitoring of Individual Doses and Assessment of Health Consequences

Both internal and external radiation doses were monitored.

Originally, x-ray films were used to measure the individual γ-ray dose received externally, but these were replaced in 1974 by radiophotoluminescent glass dosimeters and by pencil tube dosimeters worn on the body. The individual doses were originally calculated from the proton recoil tracks in a nuclear emulsion, but this practice was discontinued in 1966 because of problems associated with decay. After 1974 the individual thermal neutron doses were monitored by radiophotoluminescent glass dosimeters. All of the reactor workers exposed to long-term radiation were monitored. Ordinarily, one x-ray film reading was taken each month; the radiophotoluminescent glass dosimeters were used to record the radiation every 3 months.

The individual internal doses were determined by total-body radiation counters and by analyzing the radioactive nuclides present in urine samples. Both comprehensive and random examinations were performed, and if internal contamination was suspected, those exposed were monitored promptly. Table 1 describes the urinalysis techniques and sensitivities; the provisional maximum radiation control indices [1] and the sensitivity of the total-body counting method are also given.

Table 2 shows the radiation dose equivalents received by the reactor personnel; after 1974 the contribution from thermal neutrons is also given.

The 2,494 measurements made between 1959 and 1978 revealed a collective dose equivalent of 1537.59 man.rem. The average annual collective dose equivalent was 76.88 man•rem, with maximum and minimum doses equal to 163.63 man•rem and 34.39 man•rem, respectively. The average individual dose equivalent was 0.62 rem. Thermal neutrons were responsible for 4.1-12.1 percent of the collective dose received during 1974-1978 (the average contribution was 6.5 percent). There were eight instances altogether in which the yearly individual exposure exceeded the maximum permissible level (15.53 rem, in the worst case). There were eight instances (comprising 0.32 percent of the total number of measurements) in which the quarterly individual dose exceeded 2.5 rem. There were six accidents involving overexposure to radiation (i.e., in which more than 2.5 rem were received at one time). The accumulated dose equivalent was equal to 27.86 rem, or 1.81 percent of the total collective dose. The approximate collective dose equivalent received in accidents of all types was 44 man•rem, or 2.88 percent of the total dose. Figure 1 shows the dose distribution received by the reactor personnel during the successive years 1964-1978. The figure shows that 89 percent of the staff received less than 30 percent of the maximum permissible dose (i.e., 1.5 rem), and 64 percent received less than 10 percent (0.5 rem). The average doses before 1962 are rather high, with individual doses exceeding 1 rem per year. These doses were high because during the early years of reactor operation, the workers around the reactor and the staff manning the heavy water, helium gas, and thermoengineering systems were expected to remain present constantly at the worksite. Isotopes were actually manipulated manually and few precautions against radiation were taken. Consequently, much unnecessary exposure occurred. In addition, due to lack of

Table 1. Methods Used To Monitor Radioactive Nuclides. Sensitivity and provisional control indices.

Nuclide and type of radiation	Measurement procedure	Sensitivity	Provisional control index
Tritium	Urine samples were decolored in an activated charcoal--dextran solution and filtered through activated charcoal paper; 3 ml of the filtered urine were then mixed with 17 ml of liquid scintillator and the counts were recorded by a dual-channel liquid scintillation counter	1.6×10^{-2} μCi/l	22μCi/l (urine)
Total β-radiation	Ammonium phosphate	--	100dpm/24h (urine)
^{203}Hg	Measured by a low-α-background scintillation spectrometer with an anticoincidence shield	--	4nCi/l (urine)
^{239}Pu	A coprecipitate of bismuth and phosphoric acid was purified on an ion exchanger. The source was fabricated by electrodeposition and the radiation was recorded by a nuclear emulsion or by a low-α-background semiconductor counter	nuclear emulsion: 0.03 dpm/24h (urine). Semiconductor low-α-background counter: 0.054 dpm/24h (urine)	0.10dpm/24h (urine)
^{60}Co	Total-body counter	0.5nCi	--
^{137}Ce	Total-body counter	1nCi	--

Table 2. External Radiation Dose Equivalent Received by Reactor Personnel in Successive Years

Year	Number of workers monitored	Collective dose equivalent man•rem	Average individual dose equivalent, rem	Maximum individual dose, rem
1959	110	152.84	1.38	--
1960	121	163.63	1.35	--
1961	108	103.07	0.95	--
1962	135	71.19	0.53	--
1963	127	35.67	0.28	--
1964	135	62.11	0.46	1.99
1965	191	78.81	0.42	3.42
1966	160	66.80	0.42	4.31
1967	134	94.15	0.71	6.35
1968	136	45.53	0.33	5.10
1969	108	66.17	0.61	6.57
1970	84	61.20	0.73	4.64
1971	95	48.24	0.51	15.33
1972	98	87.61	0.89	15.53
1973	115	65.76	0.57	2.84
1974	118	43.17 (5.23) *	0.37	3.29
1975	121	65.18 (3.53)	0.54	3.94
1976	143	34.39 (2.38)	0.24	3.40
1977	130	115.02 (6.21)	0.88	4.76
1978	125	77.05 (3.18)	0.62	2.90
Total	2494	1537.59	0.62	

*) The equivalent internal collective dose of thermal neutrons is given in parentheses

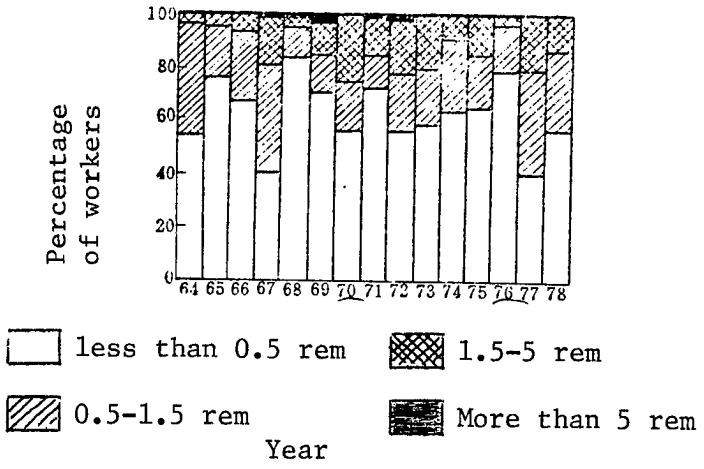

Figure 1. Distribution of Radiation Doses Received by Personnel From 1964-1978

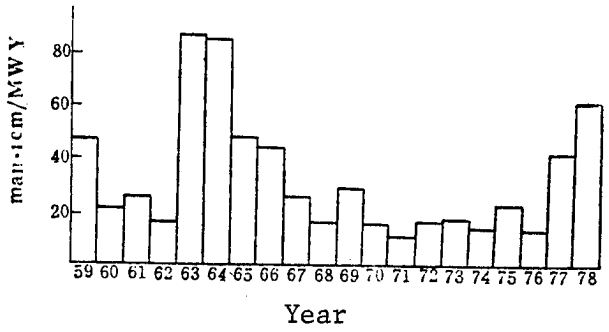

Figure 2. Dose Cost/Energy Benefit Ratio Achieved in Successive Years
The experimental values for 1959-1962 are shown to 1/10 scale.

experience the sensitivity of the x-ray film dosimetric method was not taken into account properly, and other problems such as the energy response of the film, the calibration of standard sources, etc., were ignored. All of these factors, combined with the short period of the measurements and the lack of stringent control of the conditions in the darkroom, tend to make the measured values high. After 1963, steady progress was made in operating the reactor and several procedural and technical changes were made. For example, the heavy water and other systems were inspected periodically rather than requiring workers to be continuously present; isotope samples were manipulated by remote mechanical equipment instead of manually. At the same time, procedures were tightened for controlling and monitoring the individual doses, and as a result the average dose equivalent shows a marked decline. The higher dose equivalents in the years 1972 and 1977 were the result of a radiation accident and a rod meltdown. Figure 2 shows the dose "cost" incurred during successive years per 1 MWY of energy generated by the HWRR-1. This "cost" was highest in

Table 3. Average Yearly Dose Equivalent (rem) for the Years 1967-1978

Worker category	Year 1967	1968	1969	1970	1971	1972	1973	1974	1975	1976	1977	1978	Average
Reactor core (experimental hall)	1.66	1.14	1.80	1.96	1.49	2.61	1.69	1.29	1.24	0.58	1.89	1.20	1.55
Technical supervisors	--	--	--	--	--	--	1.17	0.73	1.66	0.46	1.92	1.18	1.19
Mechanics	1.11	0.55	1.16	1.06	1.32	1.86	1.30	0.75	0.57	0.45	0.74	1.16	1.00
Chemists	0.37	0.25	0.35	0.57	0.42	0.32	0.54	0.60	1.70	0.83	1.89	0.66	0.70
Radiation protection	0.76	0.28	0.63	1.07	0.53	1.18	--	0.56	0.47	0.33	1.01	0.65	0.68
Stack workers	0.52	0.24	0.17	0.73	0.69	1.28	0.04	0.28	0.33	0.25	0.74	0.53	0.48
Heat engineers	0.66	0.32	0.25	0.47	0.31	0.71	0.37	0.22	0.34	0.39	0.47	0.28	0.40
Electricians	0.41	0.20	0.75	0.39	0.12	0.24	0.33	0.15	0.50	0.20	0.41	0.38	0.33
Physicists	0.39	0.30	0.22	--	--	--	--	--	--	--	--	--	0.30
Controllers	0.26	0.20	0.12	0.41	0.20	0.24	0.51	0.27	0.31	0.28	0.60	0.33	0.30
Operators	0.66	0.21	0.21	0.17	0.06	0.23	0.22	0.17	0.34	0.17	0.46	0.41	0.27

1959 (477.6 man·rem/MWY) and lowest in 1971 (10.2 rem/MWY). There is a 47-fold difference between the highest and the lowest yearly "costs"(corresponding to 477.6 man·rem/MWY in 1959 and 10.2 man·rem/MWY in 1971, respectively). The average "cost" during the 20 years of operation was 34.63 man·rem/MWY. Experience has shown that the "benefit"/"cost" ratio can be effectively increased by taking measures to improve radiation protection, reduce the frequency of accidents, and improve the quality of inspection and repair so that fewer inspections are needed. The ratio is also increased by operating the reactor continuously at a higher power. In Table 3 the average individual exposures received in successive years 1967-1978 are broken down according to worker category. From 1967-1978, the workers near the reactor core received a maximum average yearly individual dose of 1.55 rem (these workers were primarily responsible for removing and inserting the isotope samples in the reactor and for loading and unloading the materials). The average yearly dose of the mechanics, who were responsible for maintaining and repairing the equipment in the first reactor loop, was equal to 1.00 rem. The average yearly dose of the reactor operators who controlled the reactor was 0.27 rem, or 1/6 that of the dose received by workers stationed near the core. The reactor controllers made up 25.4 percent of the total number of workers monitored but received only 12.4 percent of the total exposure. This indicates that much of the radiation received by the workers in the heavy water reactor occurred during maintenance and repair and during isotope-manufacturing or experimental processes. Except for the contribution from neutrons, only a small fraction of the doses was received while the reactor was actually operating.

Work on internal radiation monitoring did not begin until quite late, so that no systematic data are available. Table 4 shows the tritium levels in 108 workers found from a general urinalysis carried out in 1978. The average tritium concentration was $6 \cdot 10^{-2}$ μCi/l, or 0.3 percent of the maximum permissible body burden (MPBB) [2]. The individual yearly dose equivalent 6.5mrem due to tritium was estimated from the average tritium levels in the urine samples; this value corresponds to 1.2 percent of the average external radiation dose equivalent received during the same year. In 1981 the reactor was dismantled. The spent rods were removed and immediately recut (this was formerly done using a milling cutter in a water tank, but on this occasion a lathe outside the tank was used). Due to handling errors and inadequate ventilation the worksite was accidentally contaminated. After the accident the total radioactivity was measured in urine samples taken from 25 operators, and it was found that in 9 cases the control index had been exceeded. The exposure rate 1000 dpm/24h received in the worst case was 10 times greater than the control index and was caused primarily by the nuclides ^{95}Zr, ^{95}Nb, ^{137}Cs, and ^{60}Co. In October of 1978, 113 people were examined using a total-body counter and the nuclide ^{60}Co was detected. The accumulated ^{60}Co was less than 10 nCi in 109 cases and between 10 and 15 nCi in the remaining 4 cases; the maximum level was 0.15 percent of the MPBB.

During the 17 years the reactor was in operation, 105 of the reactor personnel were medically examined and health assessments were made. No symptoms of radiation injury were found. However, the frequency of chromosomal defects and breakages in the irradiated workers was found to be higher than for the 100 who were not exposed to radiation; the total amount of glycogen in the

Table 4. Tritium Concentration in the Urine of Reactor Personnel

Worker category	Number monitored	Concentration, 10^{-2} μCi/l	
		Range	Average
Reactor core workers (experimental hall)	5	3 - 14.5	7.5
Mechanics	8	1.7 - 19.3	10.5
Radiation protection	7	1.6 - 3.0	1.9
Controllers	8	1.6 - 3.1	2.0
Chemists	6	1.6 - 45.5	17.4
Electricians	7	1.6 - 5.2	2.4
Operators	24	1.6 - 16	4.3
Heat engineers	6	2.3 - 4.3	3.3
Stack workers	16	1.9 - 15	4.1
Supervisors	3	1.8 - 5.5	3.1
Physicists	16	1.6 - 7.0	2.5
Administrators	2	1.8 - 4.0	2.9

lymphocytes was increased and the absolute number of lymphocytes circulating in the blood was elevated. In addition, there were obvious morphological changes in the neutrophil leucocytes and lymphocytes which might be attributable to occupational radiation [3].

2. Monitoring of the Worksite

The neutron and γ-radiation fields, ambient radioactive gases, particulate matter, and surface contaminants were all monitored.

(1) Radiation Measurements. The radiation fields were measured principally in terms of the equivalent neutron and γ-ray exposure rates H_n and H_γ. Both fixed and portable γ-dosimeters were used where the γ-radiation flux was high; where the flux was lower, the levels were recorded by integrating dosimeters worn by each worker. In 1975 the reactor was equipped with a horizontal experimental hatch which could be opened and closed to permit operation at 10,000 kW. Under these conditions the exposure rate H_n 1.3 m above the floor of the reactor hall generally exceeded 2.5 mrem/h and must have been even higher near the horizontal hatch. Outside the hall, H_n averaged 0.68 mrem/h in the corridor on the first floor and was less than 0.1 mrem/h in the second- and third-floor corridors and in the offices. The dose rates inside the hall from fast, moderate-energy, and thermal neutrons were in the ratio 83:13:4, and H_n/H_γ = 6.7. This indicates that neutrons were primarily responsible for the radiation in the reactor hall under normal operating conditions, and that the fast neutrons are the most dangerous. The high exposures H_n in the hall resulted mainly from the inadequate measures taken to protect against the neutrons emitted from the horizontal hatch [4].

People were continually present in the hall and in the underground chamber to record the radiation flux at fixed locations. In 1960, when the reactor was operating at 3,000 kW, the average exposure rate was 0.79 mR/h; in 1978, when

the reactor was operating at 10,000 kW, the average rate was 7.56 mR/h. Thus, although the reactor power was roughly tripled during this time, the radiation rate increased tenfold. The reasons for this are as follows: 1) more long-lived nuclides were produced by corrosion products which became radioactive; 2) due to improper management, some radioactive waste products were not promptly disposed of and were allowed to accumulate in the worksite. In 1975, when the reactor was operating at 10,000 kW, the exposure rates in the corridors and offices averaged 0.43 mR/h and 0.09 mR/h, respectively; when the reactor was shut off, these dropped to 0.28 mR/h and 0.05 mR/h, respectively. When the reactor was on, most of the γ-rays came from the horizontal hatch; by contrast, when the reactor was not running, most of the radiation in the hall was produced by accumulated radioactive products.

(2) Measurements of Radioactive Gases and Airborne Particles. Table 5 lists the methods used to measure the radioactive gases present in the air and the measurement sensitivites (3σ). Under normal conditions of reactor operation the average concentration of radioactive gases present in the air in the reactor hall, underground chamber, and other worksites was too low to be measurable using an ionization chamber detector. In 1975 the tritium concentration in the air in the reactor hall and underground chamber was measured by silica gel adsorption. The ambient levels were found to be $1.1 \cdot 10^{-10}$ Ci/l, or 2 percent of the maximum permissible concentration at the worksite. The average ambient tritium concentration in the corridors and offices was $2.5 \cdot 10^{-11}$ Ci/l, or 15 percent of the maximum concentration in the areas adjoining the radioactive worksite.

Table 5. Methods Used To Detect Radioactive Gases and Their Sensitivities

Nuclide	Method		Sensitivity, 10^{-9} Ci/l
Tritium	Ionization chamber	201	30
		701	10
	Liquid scintillator method using a silica gel adsorber		$\sim 10^{-4}$
^{41}Ar	Ionization chamber	201	5
^{133}Xe			2.5

The total β-radiation from airborne particles was recorded both continuously and by taking samples at fixed times and locations. The total β-activity was usually between 10^{-15} and 10^{-13} Ci/l; under extraordinary conditions, partial inhalation could result in levels approaching or exceeding the permissible limit. The most commonly detected nuclides were ^{60}Co and ^{131}I. In 1976, while the reactor was being dismantled for inspection and repair, the radioactivity of the precipitated dust in the reactor hall and underground chamber was measured to be 10^{-11}-10^{-9} Ci/d$\cdot$m^2; under normal operating conditions, this value was less than 10^{-11} Ci/d$\cdot$m^2.

(3) Surface Contamination Measurements. The workers' clothes, shoes, and radiation protection gear were monitored directly using surface-contamination dosimeters. The contamination level of the workclothes frequently reached 10^2-10^5 βparticles/100cm^2·2π·min. After the reactor was cleaned up in 1978, 400 articles of clothing were inspected and washed and it was found that the permissible limit of 5000 β-particles/100cm^2·2π·min was exceeded in 20 percent of the cases. The floor contamination in the reactor hall and underground chamber was measured by wiping the floors with wet cottonballs. The efficiency of this technique generally varied from 20 to 70 percent, depending on the floor material and the nature of the contaminating source. Between 1967 and 1969, when floor contamination in the reactor hall was most serious, the levels generally reached $5 \cdot 10^3$-10^6 β-particles/100cm^2·2π·min. The average level of $3 \cdot 10^5$ β-particles/100cm^2·2π·min was 10 times higher than the control level. In most cases, the contamination of the workshoes worn in the reactor hall exceeded the control index, owing mainly to the presence of ^{60}Co. The principal sources of floor contamination were: spreading of powder and dust produced by the radioactive samples; the empty rods removed from the stack after processing and left in the reactor hall; contamination of the equipment during inspection and maintenance by dripping heavy water, etc. The corridors, offices, and other locations have on occasion been partially contaminated due to the lack of strict procedures for cordoning off contaminated areas. Since ^{60}Co was the chief culprit, and standard ^{60}Co source was used to calibrate the surface contamination meters, the measured efficiency was found to be 1-3 percent.

3. Monitoring of the Three Types of Wastes

(1) Radioactive Gaseous Wastes. The radioactive gases and airborne particles emitted by the HWRR-1 were not collected and purified but were instead expelled directly from the 40m-high smokestack. Table 6 shows the total amount of β-activity in the ^{41}Ar and aerosols that were discharged. The radioactive gases were monitored continuously using an ionization chamber. The measurements revealed that under normal conditions of reactor operation, the average annual radioactivity due to the discharge of ^{41}Ar was equal to 2700 Ci, and the emission rate was 3.4 Ci/MWD. The tritium concentration was monitored continuously by silica gel adsorption during 8 months in 1975-1976; the average monthly discharge was found to be 3.3 Ci, or 40 Ci on an annual basis.

The airborne particles in the smokestack were monitored while the reactor was in operation, or while the stack was being manipulated, by taking samples and recording the radioactivity accumulated over a period of 1 day. The measurements were taken promptly after the sample was collected, and the sample was allowed to decay for 3 days. The measurements were then repeated and the concentration was deduced from the difference between the readings. The total β-activity was generally between 10^{-16} and 10^{-14} Ci/l; the average annual emission of 1.02 mCi was due primarily to the nuclides ^{60}Co and ^{131}I. If accidents are included, approximately 500 mCi of β-radioactivity was discharged in aerosol form during the years 1968-1976.

2. Radioactive Water Wastes. Prior to 1961, waste water containing less than $1 \cdot 10^{-8}$ Ci/l was discharged directly into the sewage system. After 1961 this

Table 6. Total Activity in ^{41}Ar and Aerosols Discharged From the Reactor Smokestack

Year	Average MWY	^{41}AR Ci	Total β-activity in the aerosols Concentration, 10^{-4}Ci/l Range	Average	N Discharge, mCi Excluding accidents	Accidents
1959	0.32	391				
1960	0.80	979				
1961	0.39	477				
1962	0.42	514				
1963	0.41	501				
1964	0.73	893				
1965	1.63	1995				
1966	1.55	1897	0.08-6.8	0.35	0.288	
1967	3.50	4284	0.07-3.5	0.41	0.507	
1968	2.83	3464	0.11-19	0.55	0.633	
1969	2.26	2766	0.08-1500[1)]	2.01[4)]	2.484	17
1970	3.91	4785	0.06-50	0.70	0.864	
1971	4.72	5777	0.05-18	0.47	0.583	
1972	5.14	6291	0.07-62	2.70	3.348	
1973	3.60	4406	0.12-740[2)]	3.40[4)]	4.211	400[5)]
1974	2.90	3549	0.05-8,2	0.20	0.162	
1975	2.80	3427	0.06-452[3)]	0.91[4)]	0.747	48
1976	2.55	3121	0.04-38	0.28	0.230	
1977	2.71	3317	0.19-222	1.20	0.990	20
1978	1.25	1530	0.09-180	0.48	0.396	
Totals	44.4	54000	Average; level=1.02		500	

1) The ^{76}As sample burned up
2) The ^{131}I sample ruptured and leaked
3) The ^{203}Hg sample ruptured and leaked
4) This value excludes accidents
5) Deduced from measurements of the surrounding area

practice was discontinued and waste water was either stored or sent to a water treatment facility. Initially, the total β-activity of water waste samples discharged in front of the plant was measured by evaporating the water; at present, however, both the tritium and the total β-activity are monitored using liquid scintillation counters. Table 7 describes the sources and discharge of water wastes during the years 1961-1978. During these 18 years a total volume of roughly 2,500 m^3 of water wastes was discharged (this excludes the water used for laundry and bathing); the total β-activity was approximately 500 Ci (calculated for the pure liquid), and the tritium activity was 100 Ci. An average of approximately 140 m^3 of water wastes was discharged annually, amounting to 56 percent of the rated capacity. Water wastes exceeding 10^{-4}Ci/l comprised 5 percent of the total volume but accounted for most of the radioactivity.

Table 7. Sources and Discharge of Water Wastes From 1961 to 1978

Source	Where released	Concentration range, Ci/l: Total β radiation	Concentration range, Ci/l: Tritium	Principal nuclides	Average annual discharge, m^3	Total discharge m^3
Cleaning water used for decontamination	Pit No 49	10^{-8}-10^{-4}	10^{-6}-10^{-3}	^{3}H, ^{60}Co, fission fragments	60	1080
Heavy water purification	Rooms No 28 & No 29	10^{-6}-10^{-2}	10^{-5}-10^{-2}	"	1	18
Rod milling	Hot cell	10^{-4}-10^{-1}	--	Fission fragments	--	12
Rod cooling system	Stored in a cistern	10^{-8}-10^{-4}	10^{-6}-10^{-4}	^{3}H, ^{60}Co, fission fragments	50	900
Protective water box	Inside the rector	10^{-8}-10^{-4}	10^{-6}	^{59}Fe, ^{51}Cr	25	450

(3) Solid Radioactive Wastes. Solid wastes were housed temporarily in a holding room. A volume of 240 m^3 was produced during 20 years, corresponding to an annual average of 12 m^3. Five to 10 percent of this volume consisted of discarded rods from the reactor pile, experimental pipelines, ion-exchange columns, and other intensely emitting solid wastes. Four hundred processed rods had been handled by 1978 and their surface contamination amounted to 30 Ci [^{60}Co]. Most (roughly 70 percent) of the total solid waste volume consisted of weakly emitting discarded articles, radiation protection gear, decontamination agents, garbage containers, etc.

4. Accidents

Several different types of accidents have occurred.

(1) Excessively High Accidental Exposures. One of the most serious accidents involving total-body external radiation occurred in 1972 and was caused by errors in manipulating a 200 Ci ^{60}Co sample. Altogether, four people were exposed during the accident. In the most serious case, one individual received 13.2 rem, 7.4 rem, and 6 rem in the head, chest and legs, respectively.

In 1973, a hermetically sealed tank ruptured while an ^{131}I sample was being removed from the pile and the five workers handling the sample were exposed to varying amounts of ^{131}I. It was determined afterward that 3μCi of ^{131}I was present in the thyroid of the worker receiving the most exposure; this amount corresponds to a dose equivalent of 19.4 rem [5].

(2) Accidents Involving Air Contamination. In October 1966, damage to the reactor elements caused some rubber sampling tubes to rupture, permitting 800 liters of gas (primarily ^{4}He and ^{133}Xe) to escape from inside the pile and contaminate the reactor hall (18,000 m^3). The concentration of radioactivity in the air reached $(1-5)\cdot10^{-5}$ Ci/l. The control index for ^{133}Xe at the worksite was exceeded by a factor of 1,000 and 45 Ci was released into the air. In 1973, heavy water leaked through a faulty valve while the reactor was in operation and the tritium levels at the worksite reached $1.4\cdot10^{-5}$ Ci/l, or 3,000 times the maximum permissible level. Within 2 hours, 4.4 Ci of radioactive gas was vented through the smokestack. Urine samples analyzed after the accident were found to contain 18.77 μCi/l of tritium, corresponding to an internal radiation dose equivalent of 136 mrem. In 1973, 0.4 Ci of ^{131}I was discharged into the environment in an accident involving leakage of a damaged ^{131}I sample [6]. In May 1977 a meltdown accident occurred while the system components were being tested and 1600 Ci of ^{133}Xe and 20 mCi of ^{131}I were discharged into the environment due to failure to tighten a seal in the hermetic system [7].

(3) Accidents Resulting in Spillage and Surface Contamination. An accident occurred in 1964 which contaminated a large area of the reactor hall with plutonium. Peak counts in the contaminated area (1500 m^2) reached 10^6 α-particles/100$cm^2\cdot2\pi\cdot$min. The contamination resulted from spillage of a 16 g pulverized PuO_2 target (17.6 mg, equivalent to 1.1 mCi, was estimated to have been spilled) [8]. Analysis of urine specimens collected after the accident revealed a maximum plutonium concentration of 0.257 dpm/24h, from which the radioactivity accumulated in the body was calculated to be 0.012μCi, or 31 percent of the MPBB [9]. In 1974 and 1975, a radioactive ^{203}Hg sample ruptured while being removed from the pile and spilled onto the walls and floor of the small room located at the top of the pile. The exposure rate at the hottest point reached 12 R/h. The peak ^{203}Hg concentration found in urine specimens after the accident was 17.5 nCi/l, which exceeded the control level by a factor of 4.4. The internally accumulated ^{203}Hg was measured using a total-body counter and was equal to 690 nCi in the worst case (corresponding to 17.2 percent of the MPBB) [10].

4. Accidental Discharges. In ..., 1977, contaminated mechanical components were mistakenly flushed into the industrial sewer underneath the chemistry laboratory, resulting in contamination of the sewage system. After the accident a peak exposure rate of 7.2 R/h was measured outside the walls of the sewage pipes. In this instance the radioactivity was discharged from the plant into the main industrial sewage system and detected within 24 hours after the accident.

5. Conclusions

(1) External γ-irradiation accounted for most of the dose received by workers at the HWRR-1 reactor. The average annual γ-dose equivalent was 0.62 rem, or 12 percent of the maximum permissible body burden. Except for a very few instances in which the concentration of nuclides reached or exceeded the control indices, the internal contamination was less than 1 percent of the maximum permissible accumulated dose. Comprehensive medical examinations did not reveal any diagnosable radiation-related injuries.

(2) Maintenance workers and operators manipulating the isotopes in and out of the pile received the highest amounts of radiation. For example, the maintenance workers were exposed to more radiation than were the controllers. The average "cost" in collective dose equivalent per 1 MWY over a period of 20 years was 34.63 man·rem. Radiation exposure is best reduced by strengthening radiation-protection measures, replacing manipulation by remote control, improving the quality of inspection and maintenance, and reducing the frequency of accidents.

(3) The radioactivity discharged into the environment was less than the permissible limit. Under normal conditions of reactor operation at 1 MWD, an average of 3.4 Ci of ^{41}Ar was discharged; this corresponds to a total discharge of $5.4 \cdot 10^4$ Ci over 20 years. An average of 3.3 Ci of tritium was discharged during 1975-1976. The total average annual β-activity discharged in aerosol form was 1.02 mCi, and the average yearly volume 140 m^3 of water wastes discharged contained a total radioactivity of 600 Ci. The total volume of waste material processed in the reactor was equal to 240 m^3. In order to protect the environment, the radioactive materials must be treated and purified before being discharged, particularly after an accident has occurred.

(4) The contamination levels and radiation fields inside the reactor hall were quite high and occasionally exceeded the permissible standards. Radiation protection measures must be tightened near the experimental horizontal port in the reactor and waste management should be improved to insure prompt disposal of wastes from the worksite.

(5) Cobalt-60 is one of the nuclides most seriously implicated in causing external and internal radiation. Research is necessary to find new materials which contain a higher percentage of stable cobalt and can be used as the components of the heavy water pumps.

REFERENCES

1. Individual dose monitoring group, Radiation Protection [in Chinese], 2, 1 (1982).

2. Reactor reconstruction and radiation protection group, in: Extracts From the First Technical Exchange Conf., China Nuclear Radiation Protection Association [in Chinese], Atomic Energy Publishers (1982), pp 41-46.

3. Heavy-water reactor health assessment group, Assessment of the Health of Heavy-water reactor personnel (1958-1975), Report [77]-005.

4. Leng Ruiping, et al., Measurement of the mixed n-γradiation dose in an experimental heavy-water reactor, Report [76]-005.

5. Zhang Yongxiang, Determination of the internal radiation dose in an ^{131}I contamination accident, Report [75]-018.

6. Wang Huamin, Environmental consequences of accidental discharge of ^{131}I from a heavy-water reactor, Report [75]-011.

7. Reactor reconstruction and radiation protection group, Study of radiation safety during a meltdown at an experimental heavy-water reactor, to appear (1982).

8. Zhang Yongxiang et al., An accident resulting in plutonium contamination, to appear (1982).

9. Medical protection monitoring group, Use of diethylenetetraminepentaacetic acid (DTPA) in accelerating elimination of $^{239}PuO_2$ from the human body, Report [75]-017.

10. Individual dose monitoring group, Summary of results on individual dose measurements for 1975, Report [76]-023.

CSO: 4008/91

AERIAL REMOTE SENSING FLIGHTS TO BE MADE OVER HANGZHOU BAY

Hangzhou ZHEJIANG RIBAO in Chinese 19 Apr 84 p 1

[Text] Aerial remote sensing technology will be used over Hangzhou Bay in order to carry out research work on coastal resources. All preparations for the work have now been made.

In flying remote sensing missions over the coast, remote sensing technology is employed to photograph terrain maps. In this manner, much of the field mapping work can be carried out indoors and the terrain maps produced are much more accurate than those drawn from radio bearings, and the process requires less time and labor. In remote sensing photography, targets are visible, beach features may be analyzed, complex terrain differences discerned, and the exact details of resource deposits made known. This is of vital importance in developing Hangzhou Bay.

In order to complete this remote sensing flight, the Provincial Cartographic Bureau, the Second Institute of Oceanography, and civil aviation companies have made a great deal of preparation. The Provincial Cartographic Bureau has positioned over 80 aerial photography markers along the northern and southern shores of Hangzhou Bay.

Also participating in the experiment are 9 units and the cadres and people of the 11 counties that ring the bay. Now, dozens of engineers and technicians have taken up positions on the coast and on the waters of the bay itself, ready to conduct coordinated observations as the remote sensing flights are made. A specially equipped aircraft is now sitting at the airfield awaiting orders to take off.

CSO: 4008/295

REMOTE SENSING FLIGHTS BEGIN OVER HANGZHOU BAY

Hangzhou ZHEJIANG RIBAO in Chinese 23 Apr 84 p 1

[Text] Yesterday, the "thousand-li eye" remote sensing technology really showed its stuff over Hangzhou Bay. This launched the study of coastal resources by making photographic terrain maps of Hangzhou Bay using remote sensing technology.

In the morning, this reporter rode aboard a medium passenger aircraft which carried the "thousand-li eye" as it cruised at an altitude of 5000 meters. Under the clear sky, the Jintang River looked like a band of silver, its banks warm in the spring sun. Twenty minutes later, the aircraft turned toward the skies over golden Hangzhou Bay. The air in the cabin was now thin and the temperature only 5°C; the crew had all donned their oxygen masks. The aerial camera located in the aft part of the cabin began its crucial task. Cameraman Li Mingxi explained to me: "This 'thousand-li eye' permits people to see near infrared light waves as well as objects on the ground with a resolution of 6 square meters. A picture is taken every 14 seconds, each one covering an area of almost 200 square kilometers. "The aircraft then flew over Ci Xi, Hangzhou Bay's broadest expanse of beach, and the wide beach could be seen clearly from the plane, as could the numerous marker boats with their red cloth strips. Coordinating with the observations of the personnel aboard the aircraft were workers aboard the boats who had been at sea for 3 days and nights. Yesterday, the crew of the aircraft flew for more than 6 consecutive hours over the shoreline of Hangzhou Bay, covering more than 280 kilometers and taking photographs of some 3,600 square kilometers of the coast.

CSO: 4008/301

NEW FORMULAE FOR CALCULATING MELTING TEMPERATURE, GRUNEISEN COEFFICIENT, ISOTHERMAL PRESSURE OF METALS UNDER HIGH PRESSURE

Beijing WULI XUEBAO [ACTA PHYSICA SINICA] in Chinese No 8, Aug 83, pp 1086-1092

[Article by Xie Panhai [6200 4149 3189] of the 901 Research Institute, Chengdu]

[Text] Abstract

In this paper, a new melting equation is derived. Based on this equation, a formula for calculating the Gruneisen coefficient and an isothermal equation of state are obtained by using the Lindeman equation. It is shown that the new equations are consistent with known theoretical and experimental results.

I. Melting Phenomenon

Materials under high pressure satisfy the empirical equation of Simon:

$$\frac{p+a}{a}=\left(\frac{T_m}{T_{0m}}\right)^c, \tag{1}$$

where p is pressure; T_{0m}, T_m are the melting temperatures of the material under zero pressure and high pressure conditions respectively; and a, c are constants determined from experimental data.

In Ref. [1], it has been shown that on the basis of the postulated melting condition of metals, to a first order of approximation the melting temperature is proportional to the binding energy:

$$\frac{T_m}{T_{0m}}=\frac{D}{D_0}, \tag{2}$$

where D_0, D are respectively the binding energies of metals under zero pressure and high pressure conditions. From Ref. [2], we know that

$$D_0 = p_0 v_0, \tag{3}$$

$$D = (p + p_0)v, \tag{4}$$

where v_0, v are respectively the specific volumes of metals under zero pressure and high pressure conditions; p_0 is the zero pressure binding energy per unit volume.

By substituting equations (3) and (4) into equation (2), the following melting equation is obtained:

$$\frac{T_m}{T_{0m}} = \frac{p + p_0}{p_0 \delta}, \tag{5}$$

where $\delta = v_0/v$.

Then, substituting the isothermal equation (21) from section 3 in equation (5), we obtain:

$$\frac{T_m}{T_{0m}} = \left(\frac{p}{p_0} + 1\right)^{1 - \frac{1}{2\gamma_0 + \frac{1}{3}}}, \tag{6}$$

where $\gamma_0 = \frac{B_0 \alpha}{c_V}$ is the Gruneisen coefficient of matter under zero pressure; B_0, α, c_V are the modulus of elasticity, coefficient of expansion and constant-volume specific heat respectively. Upon rearrangement, we have:

$$\frac{p + p_0}{p_0} = \left(\frac{T_m}{T_{0m}}\right)^{\frac{n\gamma_0 + 1}{6\gamma_0 - 2}}. \tag{7}$$

If we let $a = P_0$, $c = \frac{6\gamma_0 + 1}{6\gamma_0 - 2}$, then equation (7) reduces to the Simon equation. The expression of the parameter c is identical to that in the Simon equation derived by Salter [3] using the Gruneisen relation.

Therefore, once we have determined the constants a and c of the Simon equation from theoretical considerations, it is no longer an approximate formula extrapolated from experimental results; rather, it becomes a theoretically based high pressure melting equation. For practical applications, it is much easier to use than the Lindeman equation.

$$\frac{d \ln T_m}{d \ln v} = \frac{2}{3} - 2\gamma \tag{8}$$

where γ is the Gruneisen coefficient.

If the pressure p in equation (7) is replaced by the parameter δ, then

$$\frac{T_m}{T_{0m}} = \delta^{2(\gamma_0 - \frac{1}{3})}. \tag{9}$$

which is the melting equation derived by Gilvarry [4] for the condition when T_m approaches T_{0m}.

By differentiating both sides of equation (7), we obtain the slope of the melting line as:

$$\frac{dT_m}{dp} = \frac{T_{0m}}{p_0}\left(1 - \frac{1}{2\gamma_0 + \frac{1}{3}}\right)\left(\frac{p}{p_0} + 1\right)^{-\frac{1}{2\gamma_0+\frac{1}{3}}}. \tag{10}$$

The calculated values of the initial slope $\left(\frac{dT_m}{dp}\right)_{p=0} = \frac{T_{0m}}{p_0}\left(1 - \frac{1}{2\gamma_0 + \frac{1}{3}}\right)$ are in good agreement with experimental results [5], as shown in Table 1.

Table 1

(1) 材 料 / $\left(\frac{dT_m}{dp}\right)_{p=0}$	Na	Mg	Zn	Cu	Fe	Pb	Ag	Cd	Ni
(2) 实验值 ($kb^{-1}ar$)	7.8 6.5	7.5	4.5 4.8	4.2	3.0	10.0 6.6	5.5	9.0 5.6	3.7
(3) 计算值 ($kb^{-1}ar$)	4.68	5.49	3.50	3.20	2.84	6.13	4.69	3.95	2.95

Key:
1. Material
2. Experimental value ($kb^{-1}ar$)
3. Calculated value ($kb^{-1}ar$)

It can be seen that dT_m/dp decreases with increasing p, and the rate of decrease is proportional to $\left(\frac{p}{p_0} + 1\right)^{-\frac{1}{2\gamma_0+\frac{1}{3}}}$. This is consistent with the observed result that the T-p curve deviates only slightly from a straight line.

Urtiew and Grover [6] made measurements of the melting temperatures of magnesium under pressure conditions of several hundred thousand bar, and have produced a T-p curve based on the high pressure experimental data. As shown in Fig. 1, the calculated results from equation (7) are in good agreement with the experimental curve, but the extrapolated result obtained by using low pressure experimental data and the Simon equation (a = 6.4 kbar, c = 5.8) deviated significantly from the experimental values for pressures above 100 kbar.

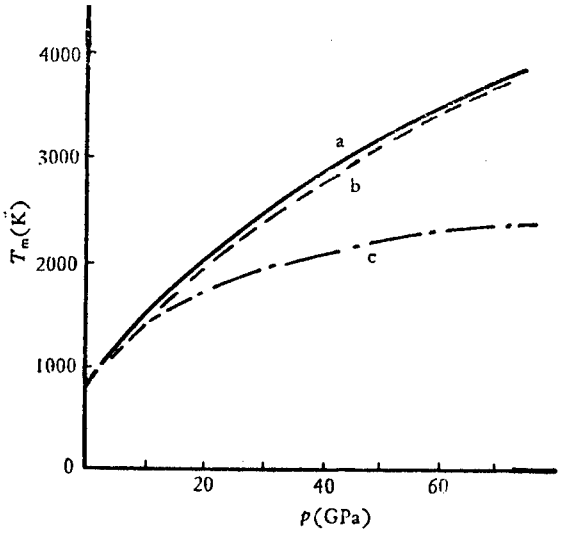

Fig. 1. Melting Curve of Magnesium. a refers to high pressure experimental curve; b refers to the calculated melting curve based on equation (7); c refers to the calculated melting curve based on equation (1)

II. Gruneisen Coefficient

The Gruneisen coefficient is an important parameter in the calculation of the equation of state. In a semi-empirical equation of state, the Gruneisen coefficient is generally computed from the following formula:

$$\gamma_t = -\left(\frac{2}{3} - \frac{t}{3}\right) - \frac{v}{2}\frac{d^2(pv^{2t/3})/dv^2}{d(pv^{2t/3})/dv}. \tag{11}$$

where t = 0, 1, 2. Under weak shockwave approximations, we have:

$$p \approx p_H = C_0^2 \frac{V_0 - V}{[V_0 - \lambda(V_0 - V)]^2}, \tag{12}$$

where p_H is the pressure of the shockwave; C_0, λ are respectively the zero pressure distance and slope of the linear approximation of the shockwave velocity D and particle velocity u. By substituting equation (12) into (11) and letting $v = v_0$, the zero pressure Gruneisen coefficient becomes

$$\gamma_t(v_0) = 2\lambda - \left(\frac{2}{3} + \frac{t}{3}\right). \tag{13}$$

Taking the logarithm of both sides of equation (5) and differentiating, we obtain:

$$\frac{d\ln T_m}{d\ln v} = \left[\frac{d\ln(p + p_0)}{d\ln v}\right] + 1. \tag{14}$$

Comparison of equations (14) and (8) yields another formula for calculating the Gruneisen coefficient:

$$\gamma^*(v) = -\frac{1}{6} - \frac{v}{2}\left(\frac{dp/dv}{p + p_0}\right). \tag{15}$$

By the same token, by substituting equation (12) into (15) and letting $v = v_0$, we obtain:

$$\gamma^*(v_0) = -\frac{1}{6} + \frac{1}{2}\left(\frac{\rho_0 C_0^2}{p_0}\right). \tag{16}$$

Substituting $p_0 = \frac{3\rho_0 C_0^2}{6\gamma_0 + 1}$ [2] into equation (16) gives

$$\gamma^*(v_0) = \gamma_0. \tag{17}$$

For certain metals, the three values $\gamma_t(v_0)$ calculated from equation (13) differ substantially from the thermodynamic γ_0, thus violating the self-consistency conditions of thermodynamics. However, if equation (15) is used to calculate the Gruneisen coefficient, then $\gamma^*(v_0)$ is self-consistent with the thermodynamic γ_0.

Calculations show that under high pressure conditions, $\gamma^*(v)$ is generally larger than $\gamma_t(v)$, as shown in Fig. 2. Of course, the use of equation (15) to calculate the Gruneisen coefficient is a new attempt; its accuracy must be verified by experimental data.

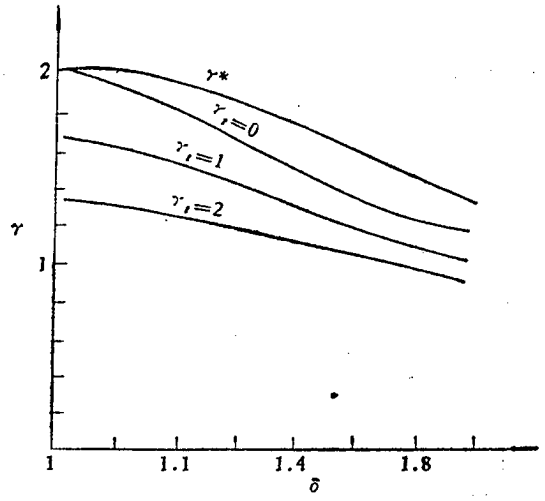

III. Isothermal Equation of State

The well-known Murnaghan isothermal equation of state is of the form:

$$p = \frac{B_0}{B_0'} (\delta^{B_0'} - 1), \tag{18}$$

where B_0, B_0' are respectively the modulus of elasticity and its first derivative under zero pressure condition. Anderson [7] pointed out that by determining the coefficients of the Murnaghan equation using ultrasonic data for pressures below 10 kbar, it is possible to extrapolate the results to a pressure range of 500 kbar without significant deviation from experimental results. In order to extend the range of applicability of the Murnaghan equation, attempts have been made to introduce second order corrections, but calculations show that the Murnaghan equation with second order correction deviates substantially from experimental results.

The Lindeman equation (8) can be integrated to give

$$T_m = T_{0m}\delta^{-\frac{2}{3}} e^{2\int_1^\delta \frac{\gamma}{\delta} d\delta}, \tag{19}$$

Comparing this equation with equation (5) yields the following isothermal equation of state:

$$p + p_0 = p_0\delta^{\frac{1}{3}} e^{2\int_1^\delta \frac{\gamma}{\delta} d\delta}. \tag{20}$$

Assume that $\gamma = \gamma_0 = \frac{B_0\alpha}{c_V}$, then

$$p + p_0 = p_0\delta^{\frac{1}{3}}\delta^{2\gamma_0},$$

If we let $P_0 = B_0/B_0'$, $B_0 = 2\gamma_0 + 1/3$, then equation (21) reduces to the Murnaghan equation.

$$p = p_0(\delta^{2\gamma_0+\frac{1}{3}} - 1). \tag{21}$$

Tables 2 and 3 present a series of p-δ relations calculated from equation (21). Each material in the table is divided into 3 to 5 rows: the 1st row refers to the experimental value of δ; the 2nd row refers to the calculated value using the method of this article; the 3rd row refers to the calculated value based on the Murnaghan equation (18); the 4th row refers to calculated value of Ref. [9] based on B_0; and the 5th row refers to the calculated value using the semi-empirical equation of state. It is seen that the values calculated from equation (21) and from the semi-empirical equation of state are in closest agreement with experimental results, whereas the values calculated from the Murnaghan equation (18) deviate the farthest from experimental results. For pressures higher than the measured experimental points, the values in row 2 and row 5 are essentially identical. Therefore, once the experimental data of the thermodynamic γ_0 and B_0 of a material

under zero pressure are known, they can be used to calculate the equation state for low-impedance materials below 1 million bar and for medium or high-impedance materials at several million bar without having to perform experiments under pressure.

Table 2

Material	B_0 (GPa)	B_0'	γ_0	n $\left(2\gamma_0+\frac{1}{3}\right)$	v0/v under pressure p(GPa)													Sequence number
					2	4	6	8	10	20	30	40	50	80	100	200	300	
Mg	36.9	5.48	1.43	3.193	1.054	1.100 1.143		1.181 1.217		1.368 1.490		1.597 1.692						1
					1.051	1.098 1.140		1.179 1.216		1.370 1.493		1.597 1.689		1.91				2
					1.049	1.089 1.123		1.154 1.181		1.286 1.363		1.571 1.475						3
					1.050	1.094 1.133		1.169 1.216		1.334 1.436		1.520 1.591						4
					1.05	1.10			1.20	1.35	1.48	1.59	1.69	1.96				5
Cd	58.0	8.49	2.26	4.853	1.036	1.068 1.096		1.122 1.145		1.241 1.316		1.377 1.431			1.631			1
					1.032	1.061 1.087		1.111 1.133		1.225 1.295		1.354 1.404			1.629			2
					1.031	1.056 1.078		1.096 1.122		1.175 1.219		1.254 1.283			1.382			3
					1.031	1.057 1.079		1.099 1.117		1.185 1.234		1.273 1.305			1.417			4
Ag	108.7	6.07	2.40	5.133	1.018	1.035 1.050		1.065 1.080		1.140 1.190		1.233 1.272			1.420			1
					1.018	1.034 1.050		1.064 1.078		1.138 1.188		1.230 1.266			1.405			2
					1.018	1.034 1.049		1.063 1.076		1.131 1.176		1.213 1.246			1.364			3
					1.018	1.305 1.051		1.066 1.080		1.144 1.198		1.245 1.286			1.445			4
Au	220.2	5.60	3.03	6.393	1.010	1.020 1.031		1.040 1.049		1.091 1.127		1.160 1.190			1.312			1
					1.008	1.017 1.025		1.040 1.041		1.074 1.103		1.128 1.151			1.237			2
					1.009	1.017 1.025		1.032 1.039		1.069 1.094		1.116 1.134			1.203			3
					1.009	1.017 1.025		1.033 1.040		1.074 1.102		1.126 1.148			1.232			4
Pb	41.6		2.46	5.253	1.042	1.078 1.110		1.139 1.166		1.274 1.361		1.433 1.495						1
					1.044	1.081 1.113		1.142 1.168		1.271 1.347		1.409 1.461			1.65			2
					1.045	1.084 1.119		1.152 1.180		1.300 1.392		1.468 1.532						4
					1.05	1.09				1.29		1.49			1.72			5
Cu	137.1		1.96	4.253	1.014	1.027 1.040		1.025 1.064		1.116 1.161		1.202 1.238			1.385			1
					1.014	1.028 1.041		1.054 1.066		1.121 1.169		1.210 1.248			1.369	1.59	1.73	2
					1.014	1.028 1.042		1.055 1.066		1.127 1.180		1.229 1.273			1.457			4
					1.014		1.05					1.21	1.24		1.39	1.59	1.73	5

Table 3

Material	B_0 (GPa)	γ_0	n $\left(2\gamma_0+\frac{1}{3}\right)$	v_0/v under pressure p(GPa)														Sequence number
				2	4	6	8	10	20	30	40	50	100	200	300	500	900	
Ni	187.5	1.91	4.153	1.010	1.020	1.030	1.040	1.048	1.091	1.127	1.161	1.192	1.319					1
				1.010	1.020	1.030	1.040	1.048	1.091	1.128	1.162	1.193	1.320	1.50	1.63	1.82		2
				1.011	1.021	1.031	1.041	1.050	1.096	1.137	1.175	1.210	1.359					4
								1.05		1.16	1.19	1.31	1.49	1.61	1.81			5
Ta	194.3	1.60	3.533	1.010	1.019	1.029	1.038	1.047	1.091	1.129	1.164	1.198	1.342					1
				1.010	1.020	1.030	1.039	1.048	1.092	1.131	1.167	1.201	1.341	1.54	1.70	1.92		2
				1.010	1.020	1.030	1.040	1.050	1.095	1.137	1.176	1.214	1.376					4
													1.36	1.56	1.71	1.93		5
W	306.7	1.54	3.413	1.007	1.012													1
				1.006	1.013					1.09					1.54	1.74	2.02	2
										1.10					1.54	1.73	2.02	5
Co	190.4	1.82	3.973	1.010	1.019	1.029	1.038	1.047	1.088	1.126	1.160	1.192	1.325					1
				1.010	1.020	1.030	1.040	1.049	1.092	1.130	1.165	1.197	1.328					2
				1.010	1.021	1.030	1.040	1.050	1.094	1.135	1.173	1.208	1.355					4
Zn	73.2	2.18	4.693	1.031	1.058	1.082	1.105	1.126	1.212	1.280	1.339	1.389	1.585					1
				1.026	1.050	1.072	1.092	1.111	1.192	1.257	1.311	1.358	1.532					2
				1.026	1.049	1.069	1.088	1.106	1.178	1.233	1.279	1.318	1.458					4
V	154.3	1.29	2.913	1.012	1.025	1.036	1.047	1.058	1.110	1.156	1.198	1.238	1.403					1
				1.013	1.025	1.038	1.049	1.061	1.116	1.167	1.213	1.256	1.439					2
				1.013	1.025	1.038	1.050	1.061	1.117	1.167	1.214	1.261	1.443					4
Na	6.6	1.25	2.833	1.245	1.412	1.546	1.664	1.767	2.183									1
				1.245	1.423	1.568	1.692	1.800	2.221									2
				1.283	1.536	1.769	1.986	2.193	3.012									4

IV. Discussion

1. Since the melting equation (7) is derived from the isothermal equation of state (21), both equations have the same range of applicability.

2. Equation (20) directly relates the isothermal pressure to the thermodynamic parameter γ, thus providing a convenient way to calculate the physical parameters of materials under high pressure such as the Debye temperature $\theta(v)$ and the isentropic unload temperature T_S

$$\theta(v) = \theta_0 e^{-\int_{v_0}^{v} \frac{\gamma}{v} dv} = \theta_0 \delta^{-\frac{1}{6}} \left(\frac{p}{p_0} + 1\right)^{\frac{1}{2}}, \tag{22}$$

where θ_0 is the Debye temperature under zero pressure.

Expressed in the form of the Gruneisen equation, we have:

$$T_S = T_h e^{-\int_{v_h}^{v} \frac{\gamma}{v} dv} = T_h \left(\frac{\delta_h}{\delta_S}\right)^{\frac{1}{6}} \left(\frac{p(v_h) + p_0}{p(v_S) + p_0}\right)^{-\frac{1}{2}}, \tag{23}$$

where T_h is the material temperature after the shockwave, v_h, v_s are respectively the shock compression specific volume and the isentropic unload specific volume $\left(\delta_h = \frac{v_0}{v_h}, \quad \delta_S = \frac{v_0}{v_S}\right)$. If $p(v) = p_0(\delta^{2\gamma_0 + \frac{1}{3}} - 1)$, then

$$\theta(v) = \theta_0 \delta^{\gamma_0}, \tag{24}$$

$$T_S(T_h, v) = T_h \left(\frac{\delta_S}{\delta_h}\right)^{\gamma_0}. \tag{25}$$

BIBLIOGRAPHY

1. Xie Panhai, WULI, 10 (1981), 612.
2. He Shouan, Xu Ji'an, WULI XUEBAO, 28(1979), 581.
3. L. Salter, PHIL. MAG., 45 (1954), 369.
4. J. J. Gilvarry, PHYS. REV. LETT., 16(1966), 1089.
5. L. Kaufman, in "Solids Under Pressure," W. Paul, D. M. Warschauer edits Acad. Pres. (1963) p 303.
6. P. A. Urtiew, R. Grover, J. APPL. PHYS. 48(1977), 112.
7. O. L. Anderson, J. PHYS. CHEM. SOLID, 27(1966), 547.
8. G. R. Barsch, Z. P. Chang, NBS SPECIAL PUBLICATION, 326(1968), 173.
9. Xu Ji'an, WULI XUEBAO, 27(1978), 342.

3012
CSO: 4008/148

BRIEFS

CHINA DEVELOPS NEW FIGHTER--Relying on its own resources, China is now developing a supersonic all-weather fighter aircraft, the "Jianji-8." This delta wing aircraft, whose fuselage is larger than the "Jian-7" (MiG 21), has a wingspan of 10 meters. The aircraft is powered by two WP-7 turbojets. The aircraft has a maximum speed of Mach 2.3, and a range of 1300 to 2000 kilometers. It is equipped with advanced radar and fire control systems. [Text] [Yinchuan NINGXIA RIBAO in Chinese 23 Apr 84 p 4--excerpted from SHANGHAI YIBAO]

UNDP CONCRETE COURSE IN HANGZHOU--Hangzhou, 4 May (XINHUA)--A seminar-workshop on prestressed concrete technology for the Asian-Pacific Region closed here today after 33 days. Fifteen trainees from Bangladesh, Malaysia, Nepal, the Philippines, Thailand, and China received their certificates for the study. Beginning on 2 April, they studied the design, production, and use of small and medium-sized prestressed concrete pieces and became acquainted with the techniques China uses to make low-cost building materials. The seminar-workshop was jointly sponsored by the UN Development Program, the UN Industrial Development Organization, and two relevant Chinese units. [Text] [OW041738 Beijing XINHUA in English 1457 GMT 4 May 84]

CSO: 4010/81

LIFE SCIENCES

HBcAg SYNTHESIZED, APPLIED TO HEPATITIS DIAGNOSIS

Beijing JIEFANGJUN YIXUE ZAZHI [MEDICAL JOURNAL OF CHINESE PEOPLE'S LIBERATION ARMY] in Chinese No 1, 20 Feb 84 pp 1-5

[Article by Ma Xiankai [7456 6343 0418], Luo Qinghua [5012 3237 5478] and Li Anli [2621 1344 7787], et al., all of the Institute of Basic Medical Sciences, Academy of Military Medical Sciences: "Synthesis of HBcAg in E. coli and Its Application in Diagnosis of Viral Hepatitis B"]

[Summary] HBcAg was synthesized in E. coli using recombinant DNA technology. The antigen in crude bacterial lysate was a satisfactory diagnostic reagent when used in ELISA for detecting antibodies to HBcAg in serum samples. It correlated well with results obtained by using HBcAg extracted from human liver and those from the corresponding Abbott kit. When compared with the routine laboratory diagnostic test using only RPHA for HBsAg, it gave 8.9 percent and 16.5 percent higher positive cases (serum dilution 1:100) in screening samples from 2040 blood donors and 158 clinically suspected hepatitis patients respectively. The crude antigen can be purified by one step affinity chromatography separation.

9717
CSO: 5400/4136

AUTHOR: CHEN Yikai [7115 6318 6946]
BAO Youdi [0545 1635 6611]
CAI Zhuqin [5591 3796 2953]
YU Enshu [0060 1869 1659]

ORG: CHEN, CAI and YU all of the Fujian Research Institute of Epidemic Diseases, Fuzhou; BAO of Fujian Medical College, Fuzhou

TITLE: "Detection of VW Antigen-associated Plasmic DNA of *Yersinia enterocolitica*"

SOURCE: Beijing ZHONGHUA WEISHENGWUXUE HE MIANYIXUE ZAZHI [CHINESE JOURNAL OF MICROBIOLOGY AND IMMUNOLOGY] in Chinese No 6, Dec 83 pp 395-397

TEXT OF ENGLISH ABSTRACT: The modified version of Eckhardt's micro-electrophoresis method was applied to the study of the correlation between plasmid DNA and VW-antigen of *Y. enterocolitica*. A total of 53 strains containing 0:3 antigen factor, isolated from humans, pigs, rats and chickens in the same area, was examined. Among them, all 52 strains with VW-antigen possessed a plasmid zone of 39.5-45.0 megadalton. However, the same plasmid was not seen in their homologous strains in the form of a non VW-antigen. These facts show that the production of a virulence determinant VW-antigen of *Y. enterocolitica* is related to 39.5-45.0 megadalton plasmid.

9717
CSO: 4009/80

END